Feedback interactions between MKP3 and ERK MAP kinase control *scleraxis* expression and the specification of rib progenitors in the developing chick somite

Terence Gordon Smith[1], Dylan Sweetman[1], Margaret Patterson[1], Stephen M. Keyse[2] and Andrea Münsterberg[1],*

[1]School of Biological Sciences, University of East Anglia, Norwich NR4 7TJ, UK
[2]CRUK Molecular Pharmacology Unit, Biomedical Research Centre, Level 5, Ninewells Hospital, Dundee DD1 9SY, UK
*Author for correspondence (e-mail: a.munsterberg@uea.ac.uk)

Summary

Cells in the early vertebrate somite receive cues from surrounding tissues, which are important for their specification. A number of signalling pathways involved in somite patterning have been described extensively. By contrast, the interactions between cells from different regions within the somite are less well characterised. Here, we demonstrate that myotomally derived FGFs act through the MAPK signal transduction cascade and in particular, ERK1/2 to activate *scleraxis* expression in a population of mesenchymal progenitor cells in the dorsal sclerotome. We show that the levels of active, phosphorylated ERK protein in the developing somite are crucial for the expression of *scleraxis* and *Mkp3*. MKP3 is a dual specificity phosphatase and a specific antagonist of ERK MAP kinases and we demonstrate that in somites *Mkp3* transcription depends on

the presence of active ERK. Therefore, MKP3 and ERK MAP kinase constitute a negative feedback loop activated by FGF in sclerotomal progenitor cells. We propose that tight control of ERK signalling strength by MKP3 is important for the appropriate regulation of downstream cellular responses including the activation of *scleraxis*. We show that increased or decreased levels of phosphorylated ERK result in the loss of *scleraxis* transcripts and the loss of distal rib development, highlighting the importance of the MKP3-ERK-MAP kinase mediated feedback loop for cell specification and differentiation.

Key words: FGF signalling, Chick, Somite, Tendon, Rib, Mkp3, ERK MAP kinase, Scleraxis

Introduction

During vertebrate embryogenesis, epithelial somites are generated sequentially from pre-segmented paraxial mesoderm (psm). In amniotes, somites are patterned by signals from the notochord, neural tube, surface ectoderm and lateral plate to give rise to the dermomyotome and the sclerotome. The definitive myotome forms from the dermomyotome (Buckingham, 2001).

Signalling between different somite compartments results in further patterning and it has been shown that growth factors from the myotome are important for the specification of sclerotome derived cell lineages, including ribs and tendons (Brent et al., 2003; Huang et al., 2003; Tallquist et al., 2000). Detailed clonal analysis of avian somites has revealed the origin of proximal and distal ribs (Evans, 2003). Furthermore, ablation experiments suggested that the mesenchymal cells at the rostral and caudal edges close to the dermomyotome, which express the bHLH transcription factor *scleraxis*, contain distal rib progenitors (Hirao and Aoyama, 2004). *Scleraxis* marks a subpopulation of sclerotomal cells and is involved in regulating gene expression within mesenchymal cell lineages that give rise to cartilage and connective tissues (Cserjesi et al., 1995; Schweitzer et al., 2001). In maturing somites, *scleraxis* marks

axial tendon progenitors in the dorsal sclerotome and it has been postulated that myotome-derived fibroblast growth factor (FGF) signals are required to activate *scleraxis* expression by an indirect mechanism (Brent et al., 2003). Recent work has implicated the Ets domain transcription factors Pea3 and Erm in the regulation of *scleraxis* expression (Brent and Tabin, 2004). This demonstrates that close interactions between the myotome and sclerotome are pivotal for the emergence of a discrete population of *scleraxis* positive cells within the somite.

We were interested in investigating further the role of the FGF signalling pathway in the specification of *scleraxis* positive somite progenitors. We have previously identified a role for the dual specificity phosphatase, MKP3, in negatively regulating the ERK MAP kinase pathway in limb and early neural development (Eblaghie et al., 2003) and this new study focuses on the function of this pathway in somite patterning and cell specification.

Mitogen-activated protein kinase (MAP kinase) cascades are effectors for many growth factor signals implicated in developmental processes, including appendage outgrowth and organogenesis. The 'classical' Ras/MAP kinase cascade in which extracellular signal regulated kinases (ERK1 and ERK2) are activated by phosphorylation of the T-X-Y motif within the

activation loop of the kinase is a major effector of signalling in mammalian cells (Kouhara et al., 1997). The developmental outcome of ERK signalling relies, at least in part, on the competing actions of upstream activators and inhibitory MAP kinase phosphatases (MKPs). Indeed, the level of FGF signalling has been suggested to play a deterministic role in cell fate and survival in a number of different systems (Hajihosseini et al., 2004; Partanen et al., 1998; Storm et al., 2003; Sato and Nakamura, 2004; Tsang et al., 2004).

The dual-specificity MAP kinase phosphatase, MKP3 (also known as PYST1), is a specific and potent regulator of the ERK class of MAP kinases (Groom et al., 1996; Muda et al., 1996). This specificity for the ERK 1/2 MAP kinases is mediated by specific protein-protein interaction and subsequent ERK-dependent catalytic activation of MKP3 (Camps et al., 1998; Muda et al., 1998). We have previously isolated the chicken and mouse orthologues of *Mkp3* and studied their embryonic expression. We found dynamic patterns of *Mkp3* messenger RNA expression in important signalling centres and known sites of FGF/FGF receptor signalling, which are associated with cell proliferation and patterning in developing mouse and chick embryos (Dickinson et al., 2002; Eblaghie et al., 2003).

We demonstrate that in differentiating somites *Mkp3* is expressed in *scleraxis*-positive progenitor cells. This expression is regulated by FGF signalling via the classical ERK MAP kinase pathway. During somite patterning, MKP3 regulates ERK MAP kinase activity by dephosphorylation demonstrating that this enzyme is part of a negative feedback loop controlling the levels of phosphorylated ERK (dpERK) in this tissue. Finally, we show that decreasing or increasing the levels of dpERK in chick somites, by mis-expression of human MKP3 or a constitutively active MEK1, respectively, results in loss of *Mkp3* and *scleraxis* expression and affects rib formation. We propose that the tight regulation of dpERK levels is crucial for the activation of *scleraxis* expression and we show that FGF signalling is important for the specification of distal rib precursors in somites.

Materials and methods

Probes and in situ hybridisation

Probes for in situ hybridisation were as described previously (Eblaghie et al., 2003) for *Mkp3*; (Schweitzer et al., 2001) for *scleraxis*; (Minowada et al., 1999) for *sprouty2*; (Niswander et al., 1994) for *Fgf8* and *Fgf4*. In situ hybridisation was essentially as described previously (Schmidt et al., 2000); however, proteinase K treatment was omitted. After the staining reaction, embryos were de-stained in high detergent mix, 5×TBST (for 100 ml of a 10× solution: 8 g NaCl, 25 ml 1 M Tris-HCl pH 7.5, 0.2 g KCl, 10 ml Tween-20) to reduce background.

Immunohistochemistry and ISH on sections

To detect myosin heavy chain protein with MF-20 antibody (Developmental Studies Hybridoma Bank) and transcripts for *Mkp3*, *sprouty2* or *scleraxis*, we performed in situ hybridisation with immunohistochemistry in combination. We followed the method described previously (Edom-Vovard et al., 2001). The proteinase K step was omitted and replaced with 0.1% Triton-X 100 15 minutes at room temperature. NBT/BCIP colour reaction was enhanced with 10% polyvinylalcohol (Sigma). *Scleraxis* transcripts were detected with Fast Red under a coverslip at 37°C. Sections were incubated with MF-20, 1/1000 dilution overnight at 4°C and detected with an 'Alexa' secondary fluorescent antibody (488 nm, Molecular Probes).

FGF and pharmacological inhibitor beads

Heparin beads (Sigma H-5263) were soaked for 1 hour at room temperature in recombinant FGF (R&D Systems) at the following concentrations: FGF4 (50µg/ml), FGF8 (1mg/ml) and FGF2 (400µg/ml). AG-1 X2 beads (BioRad) were incubated in one of the following pharmacological inhibitors: SU5402, from 5 to 10 mM; SB203580 and LY294002 both 20 mM, all from Calbiochem; and PD184352, 20 mM (a gift from Philip Cohen, Dundee) (Davies et al., 2000). All compounds were dissolved in DMSO. Beads were soaked for 1 hour at room temperature in the dark then washed twice in PBS and implanted adjacent to cervical somites of HH13 embryos or adjacent to forelimb or flank level somites of HH17 embryos. In addition, PD184352 or DMSO controls were diluted 1/10 with PBS and injected directly into thoracic somites. Embryos were fixed in 4% paraformaldehyde and processed for in situ hybridisation 1, 5 or 24 hours after the operation.

Chick embryo manipulations and constructs

Fertile chicken White Leghorn eggs were obtained from Needle farm (Sussex) and incubated at 37.5°C until the desired Hamburger-Hamilton stage was reached. Electroporation was performed in ovo using a TSS20 Ovodyne Electroporator (Intracel, UK). Expression plasmids for hMKP3-GFP, hMKP3$^{\Delta KIM}$-GFP, caMEK1 (=MKK$^{E/E}$), sFREK:Fc and dnFgfR1c have been described previously (Eblaghie et al., 2003; Marics et al., 2002; Yang et al., 2002; Cowley et al., 1994). Most plasmids encoded GFP fusion proteins or produced GFP from an IRES. Alternatively, a GFP expression plasmid was co-electroporated to mark transfected somites. Positive electrode was platinum and negative electrode was sharpened tungsten wire. Eggs were windowed and black ink was injected underneath the blastoderm to visualise the embryos. DNA (3 mg/ml in water) was injected underneath the myotome of flank somites at HH18-20, electrodes were placed on either side of the embryo and 40 V were applied for 50 mseconds, with 5 pulses spaced 500 mseconds apart. For RCAS-mediated gene expression, concentrated virus was injected into presegmented mesoderm. RCAS-sFREK:Fc has been described previously (Marics et al., 2002). The spread of infection was examined using a gag antisense probe. Eggs were sealed and incubated for the times indicated and processed for in situ hybridisation, Alcian Blue staining, western analysis or RNA extraction.

Western blots

hMKP3-GFP encodes a fusion protein, caMEK1 was co-electroporated with a GFP expression plasmid. GFP-labelled somites were pooled, protein was extracted using standard protocols (NP-40 lysis buffer with protease and protein phosphatase inhibitors, Roche), equal amounts were loaded on 10% polyacrylamide gels. Primary antibodies were applied overnight at 4°C, excess was washed and secondary antibodies coupled to HRP (Jackson Laboratories) were applied for 1 hour at room temperature. Primary antibodies used: dpERK (Cell Signaling); anti-GFP, (Clontech); and α-tubulin (SIGMA).

RT-PCR

RNA was harvested from GFP-expressing somites. cDNA was prepared using random hexamer primers as described previously (Münsterberg et al., 1995). cDNA (1 µl) was used in PCR reactions, human MKP3-GFP (30 cycles), chick Mkp3 (35 cycles), scleraxis (30 cycles) and GAPDH (25 cycles) (Münsterberg et al., 1995). Primers for chick *scleraxis*: forward, 5′-ACGTGAATTCCACACACACC-GAACCACGGAC-3′; reverse, 5′-ACGTGAGCTCATTATACGAAC-TGCTCAGGC-3′. Primers specific for human MKP3-GFP fusion: forward, 5′-ACGTCCATGGTAGATACGCTCAGACCCG-3′; reverse, 5′-ACGTAAGCTTTTACTTGTACAGCTCGTCC-3′. Specific primers for chick *Mkp3*: forward, 5′-ACGTGCGGCCGCATGCTAGATACG-TTCAGACCCGTC-3′; reverse, 5′-ACGTGAATTCTCACGTGGAC-TGCAGGGAGTCCACC-3′. Specificity of MKP3 primers was tested

on 1 ng of plasmid template. Amplification conditions for plasmid and cDNA: denaturation at 94°C for 5 minutes, followed by 30 to 35 cycles of 94°C for 30 seconds, annealing temperatures of 60°C and 55°C for both hMKP3-GFP and cMkp-3 and for scleraxis, respectively for 30 seconds and 72°C for 2 minutes. A 5 µl sample of the 30 µl reactions was analysed on a 1-2% agarose gel.

Results

### *Mkp3* transcripts co-localise with *scleraxis* in developing somites

Whole-mount in situ hybridisation demonstrated that *Mkp3* was expressed in a number of regions known for FGF signalling activity, including developing somites. Transcripts were first detected in paraxial mesoderm of Hamburger-Hamilton (HH) stage 15 embryos (Hamburger and Hamilton, 1951). High levels of *Mkp3* transcripts were expressed in the posterior half of the psm and the tail bud. Expression was diffuse in epithelial somites and then detected in a triangular shaped region abutting the neural tube as somites matured (Fig. 1A,J). As somites continued to differentiate, *Mkp3* expression became restricted to anterior and posterior somite edges giving rise to a 'twin-stripe' pattern (Fig. 1A; Fig. 2G,H). This latter pattern persisted throughout development until at least HH28 (data not shown). A detailed comparison to other known somite differentiation markers revealed that *Mkp3* transcripts correlated with transcripts of the bHLH gene *scleraxis*. Using our protocol, we could detect expression of *scleraxis* in epithelial somites at HH15 (Fig. 1K; red arrow in Fig. 1B) similar to *Mkp3* and earlier than reported previously (Brent et al., 2003). In more mature somites, *scleraxis* transcripts became restricted to anterior and posterior somite edges (Fig. 1B). Another known negative regulator of FGF signalling, sprouty2, was also expressed along the anterior and posterior somite edges giving rise to a broad stripe (Fig. 1C). In addition, sprouty2 was expressed in a thin stripe in the centre of each somite (Fig. 1L). Immunohistochemistry combined with in situ hybridisation on frontal sections confirmed that *Mkp3* transcripts were localised in the

dorsal sclerotome region where *scleraxis* transcripts were found (Fig. 1D,E). Two somites contributed to one domain of *Mkp3* expression, as shown for *scleraxis* (Brent et al., 2003). Sprouty2 was also expressed along somite boundaries (Fig. 1F). The somitic expression of *Mkp3* was associated with the appearance of *Fgf4* and *Fgf8* transcripts within the myotome (Fig. 1G,H). We found that the expression of *Mkp3* and *scleraxis* in progenitor cells along the anterior and posterior somite edges was more closely associated with the first appearance of *Fgf8* transcripts. Two FGF receptors, CEK1 and FREK are also expressed broadly in developing somites (Fig. 1I; data not shown). This pattern suggested that MKP3 is involved in modulating the FGF mediated regulation of *scleraxis* and thus could play a role for the specification of *scleraxis*-positive progenitor cells in the somite.

In somites *Mkp3* expression is regulated by FGFs and depends on active ERK MAP kinase

FGFs have previously been shown to induce ectopic expression of *Mkp3* in the neural plate and limb bud mesenchyme (Eblaghie et al., 2003). In order to determine whether FGFs were sufficient to activate *Mkp3* expression in paraxial mesoderm, we grafted beads soaked in FGFs to the dorsal somite. At stage HH13, FGF4 beads induced very high levels of ectopic *Mkp3* transcripts in somites (Fig. 2A). Similarly, FGF2 and FGF8 beads caused ectopic *Mkp3* expression (data not shown). Transverse sections showed high levels of *Mkp3* transcripts throughout somite tissue (Fig. 2B). Beads soaked in FGF10, which belongs to a separate subgroup of FGF ligands based on receptor specificity, did not induce *Mkp3* expression.

Fig. 1. Expression of *Mkp3* during chick somite development correlates with the expression of *scleraxis* in somites and with the expression of *Fgf4* and *Fgf8* in myotomes. (A-C,G-L) Whole-mount in situ hybridisation of HH15, HH19, HH20 and HH23 chick embryos. (A,J) *Mkp3*. (J) Hind-limb buds were removed to show expression in posterior somites. (B,K) *scleraxis*, blue asterisk indicates the axial level of expression in somites, red arrow indicates *scleraxis* expression in presegmented mesoderm; (C,L) *spry2*; (G) *Fgf4*; (H) *Fgf8*; and (I) *FGFR4/FREK*. (D-F) Frontal sections through HH24 somites stained with MF20 antibody to visualise myosin heavy chain protein in the myotome (green) together with (D) *Mkp3* transcripts (dark purple) in the dorsal sclerotome along the anterior and posterior somite edges. (E) MF20 and *scleraxis* transcripts (red). (F) MF20 and *spry2*. Brackets in J,G indicate the triangular shaped expression in posterior somites. ba, branchial arches; dm, dermomyotome; is, isthmus; lb, limb bud; my, myotome; ol, olfactory epithelium; op, optic vesicle; ot, otic vesicle; s, somite; sc, sclerotome; tb, tail bud.
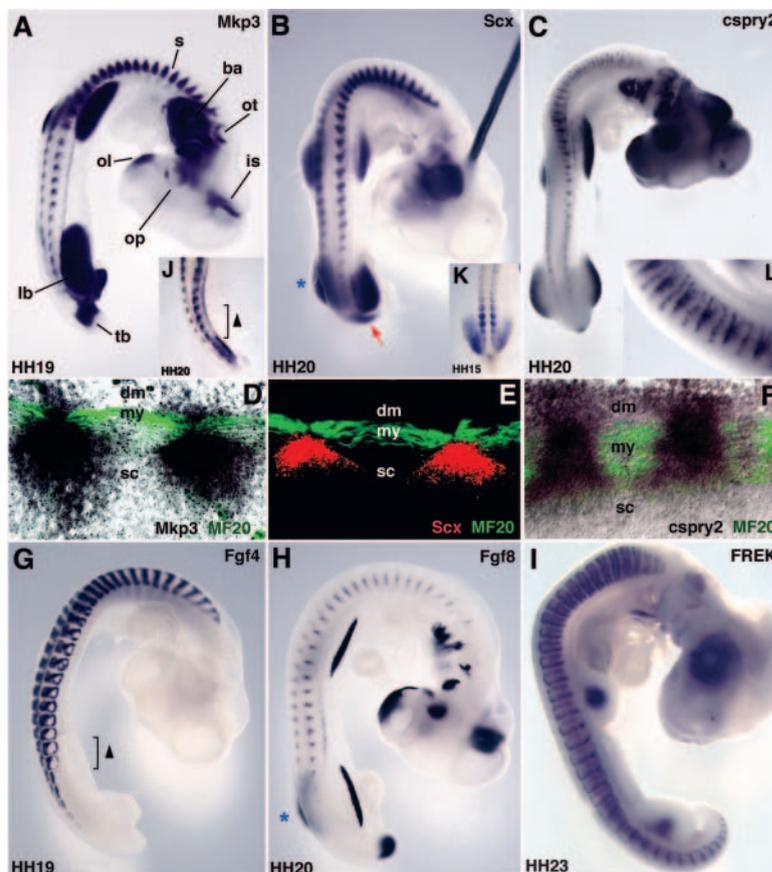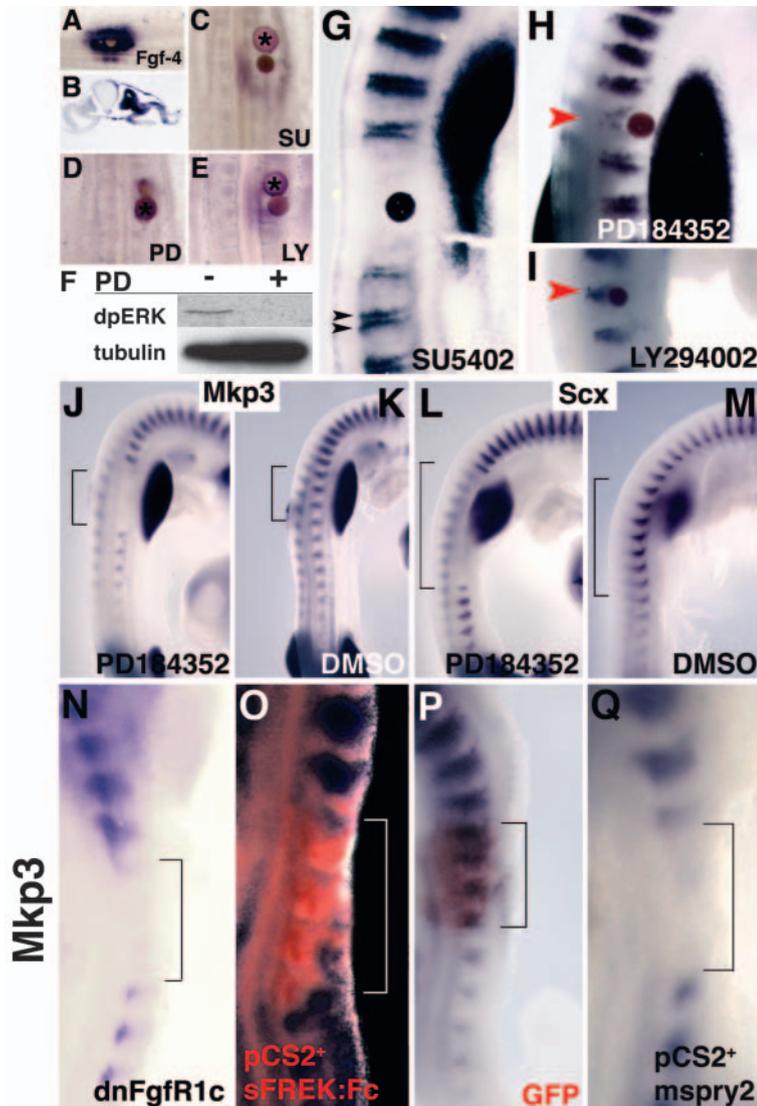
Fig. 2. FGFs regulate *Mkp3* transcripts through ERK MAP kinase in the dorsal sclerotome. (A-E) Whole-mount in situ hybridisation with *Mkp3* following FGF4 bead grafts. (A) HH13 embryo, (B) transverse section through the trunk of an HH15 embryo, showing ectopic transcripts throughout somite tissue, (C-E) *Mkp3* expression after FGF and pharmacological inhibitor bead implants, indicated by asterisks. (C) SU5402 (*n*=3/4), (D) PD184352 (*n*=8/8) and (E) LY294002 (*n*=8/10). (F) Western blot probed with anti-phospho-ERK antibody and tubulin. Protein isolated from untreated somites (–) or somites dissected after exposure to PD184352 beads (+). (G) SU5402 bead implants resulted in reduced endogenous *Mkp3* expression (*n*=7/7). Double arrowheads indicate the 'twin-stripe' expression of *Mkp3*. (H,I) PD184352 bead implants (H) resulted in reduced endogenous *Mkp3* expression (red arrowhead *n*=11/16), whereas a bead soaked in LY294002 (I) did not have any effect (red arrowhead *n*=19/19). (J,K) In situ hybridisation for *Mkp3* after injection of (J) 2 mM PD184352 into somites (*n*=15/15) or (K) DMSO (*n*=10/10). (L,M) Whole-mount in situ hybridisation for *scleraxis* after injection of (L) 2 mM PD184352 into somites (*n*=12/13) or (M) DMSO (*n*=10/10). Brackets in J-M show injected somites. Bead grafts and inhibitor injections were analyzed after 5 hours. (N-Q) FGF receptor and ERK MAP kinase activity is required for *Mkp3* expression in somites. Whole-mount in situ hybridisation of chick *Mkp3* after electroporation of a FGFR1c-EYFP fusion construct (*n*=5/5) (N), of pCS2⁺ encoding a FREK:Fc fusion protein (*n*=5/10) (O), or of pCS2⁺ encoding mouse *Spry2* (*n*=10/15) (Q). (O) Expression of sFREK:Fc is detected using a probe against the Fc domain (red). (P) Electroporation of EGFP expression vector alone (*n*=11/11). GFP transcripts were detected by in situ hybridisation (red). Brackets indicate electroporated somites.

effect (Fig. 2H; data not shown). In order to confirm in vivo the effect of PD184352, which inhibits MKK upstream of ERK, the somites beneath the bead were dissected, protein was extracted and analysed by western blot for the presence of dpERK. We observed the complete loss of dpERK in the presence of a PD184352 bead compared with readily detectable levels in untreated somites (Fig. 2F). Injection of PD184352 directly into somites resulted in complete loss of *Mkp3* transcripts, while injection of DMSO had no effect (Fig. 2J,K). Thus, endogenous expression of *Mkp3* was dependent on the presence of active, phosphorylated ERK MAP kinase and the residual expression observed in Fig. 2H is most likely due to the limited diffusibility of PD184352.

In somites, FGFs induce *scleraxis*, possibly by activating the Ets domain transcription factor Pea3 (Brent and Tabin, 2004). Therefore, we asked whether *scleraxis* expression was dependent on dpERK and found that injection of PD184352 resulted in loss of detectable transcripts (Fig. 2L,M). To corroborate these findings, somites of HH18 embryos were electroporated with a plasmid encoding a dominant-negative FGF receptor where the cytoplasmic tyrosine kinase domain had been replaced with EYFP (Fig. 2N). We also used a vector encoding a secreted extracellular domain of FREK (cFGFR4) fused to the immunoglobulin Fc domain, which mediates dimerisation (Fig. 2O). Both of these mutant receptors have previously been shown to inhibit FGF-mediated signalling (Marics et al., 2002; Yang et al., 2002), even though they probably do not discriminate between different FGF receptors

However, FGF10 beads could initiate formation of an ectopic limb bud (data not shown). Experiments using beads soaked in the FGF receptor inhibitor, SU5402, demonstrated that ectopic upregulation of *Mkp3* expression required receptor tyrosine kinase activity (Fig. 2C). Furthermore, blocking ERK MAP kinase activity or PI3 kinase activity with PD184352 or LY294002, respectively, prevented induction of ectopic *Mkp3* transcripts by FGF beads (Fig. 2D,E). Placing a bead soaked in DMSO next to an FGF4 bead had no effect (not shown).

This showed that FGFs known to act on mesenchymal cells were sufficient to induce ectopic *Mkp3* transcripts via either ERK or PI3-kinase. Next, we wanted to investigate whether FGF signalling was necessary to regulate the expression of *Mkp3* in the dorsal sclerotome. Application of a bead soaked in SU5402 led to a dramatic loss of *Mkp3* transcripts beneath the bead (Fig. 2G). A bead soaked in LY294002 did not affect endogenous *Mkp3* expression in contrast to ectopic *Mkp3* expression, which was sensitive to PI3-kinase inhibition (Fig. 2I,E). By contrast, a bead soaked in the ERK MAP kinase inhibitor PD184352 did result in a significant loss of endogenous *Mkp3* transcripts, while DMSO beads or pharmacological inhibitors that blocked other pathways had no

and receptor isoforms. Expression of both these constructs by targeted electroporation into somites resulted in loss of *Mkp3* expression in this tissue (Fig. 2N,O). By contrast, electroporation of a GFP vector alone had no effect (Fig. 2P). In addition, when we expressed the murine orthologue of sprouty2, which has been shown to inhibit the FGF MAPK pathway at the level of Ras and MEK (Hanafusa et al., 2002; Sasaki et al., 2003), we also observed a loss of *Mkp3* expression (Fig. 2Q). Together, these experiments show that somitic expression of *Mkp3* depends on FGF receptor-mediated signalling via phosphorylated ERK MAP kinase.

The response of *Mkp3* to FGF beads over time illustrates a negative feedback interaction

To demonstrate that MKP3 is part of a negative-feedback loop regulating the levels of dpERK in somites, we examined the dynamics of MKP3-dpERK interactions in embryos. We looked at both the induction of *Mkp3* expression and the levels of dpERK in response to FGF beads over time. Exposure of HH17 somites to FGF2, FGF4 or FGF8 resulted in high-level ectopic expression of *Mkp3* within 1 hour, reaching a maximum at 5 hours (Fig. 3A,B; data not shown). Transcripts were seen in all somite regions (Fig. 3F). Interestingly, after an exposure of 24 hours, we noted a clear loss of endogenous *Mkp3* transcripts in the vicinity of the beads. Ectopic expression immediately around the bead was still detectable, suggesting that active FGF was released from beads at these later time points (Fig. 3C). We next examined how the initial induction and following loss of *Mkp3* transcripts correlated with levels of active ERK by western analysis of dissected somites at the same time points (Fig. 3D). After exposure for 1 hour to FGF4, the levels of dual phosphorylated ERK were significantly increased compared with control somites. However, after a 5 hour exposure the levels of dpERK were reduced to the same levels as in control somites, most probably owing to the increased levels of MKP3 protein produced from the ectopic transcripts within the somite at this point. After 24 hours, dpERK was no longer detected, even though the levels in untreated somites had increased. This correlated extremely well with the apparent inhibition of *Mkp3* expression by FGFs after 24 hours. Interestingly, increased levels of *scleraxis* transcripts were only detected after 5 hours of exposure to an FGF bead and these were more restricted to the sclerotome compartment (Fig. 3E,G). This is consistent with observations by others (Brent et al., 2003; Brent and Tabin, 2004) and in addition indicates differences between *Mkp3* and *scleraxis* transcriptional regulation and the competence of cells to express these genes.

MKP3 regulates its own transcription by controlling the levels of active ERK MAP kinase in developing somites

In the following experiments, we investigated the function of MKP3 for transcriptional regulation and cell specification in developing somites. We transfected somites with an expression construct encoding a human MKP3 EGFP fusion protein [hMKP3-GFP; previously known as Pyst1-EGFP (Eblaghie et al., 2003)]. Somites were identified by GFP fluorescence, dissected and the levels of dpERK were analysed by western blot. This showed readily detectable levels of dpERK protein in untreated somites or in somites electroporated with empty EGFP vector (Fig. 4A, lanes 1,2). However, hMKP3-GFP
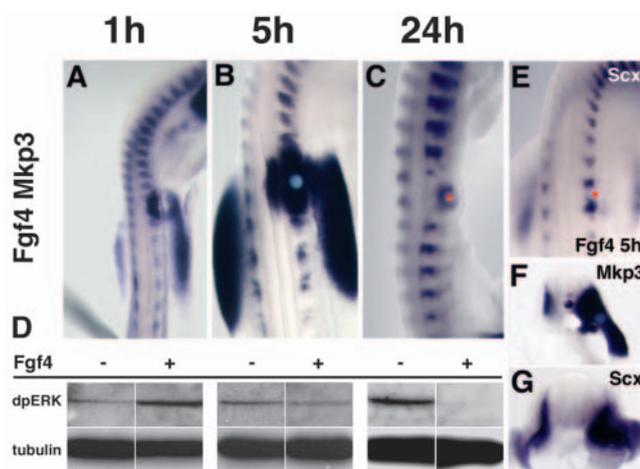

Fig. 3. The expression of *Mkp3* over time correlates with differential levels of phosphorylated ERK in response to FGF bead implants. (A-C) Whole-mount in situ hybridisation of *Mkp3* in chick embryos with FGF bead grafts, harvested after a 1-hour (A), 5-hour (B) or 24-hour exposure (C). (D) Western blot of untreated somites (–) or somites exposed to an FGF4 bead (+), harvested at the times indicated and probed with anti-phospho-ERK and α-tubulin antibodies. (E) *scleraxis* was induced by an FGF4 bead after 5 hours. (F,G) Sections demonstrating the distribution of ectopic transcripts after bead grafting, (F) *Mkp3* and (G) *scleraxis*. Red asterisks in C,E indicate the bead.

expression resulted in a loss of dpERK (Fig. 4A, lane 3). Next, we used human and chick specific primers to determine the levels of *Mkp3* transcripts in electroporated somites by RT-PCR. Specificity of the two primer pairs was confirmed against plasmid template (Fig. 4B). PCR performed on cDNA obtained from electroporated somites showed that chick *Mkp3* transcripts were present in somites, which expressed the empty EGFP vector (Fig. 4C, lane 1). However, hMKP3-GFP expression resulted in a complete loss of endogenous chick *Mkp3* transcripts. In addition, the levels of *scleraxis* transcripts were reduced significantly as a result of hMKP3-GFP overexpression (Fig. 4C, lane 2).

Immunohistochemistry on frontal sections of HH24 embryos showed that high levels of dpERK protein were readily detected in the rostral part of each somite in neural crest derived dorsal root ganglia (DRG), consistent with previous reports in mouse embryos (Corson et al., 2003). Phosphorylated ERK MAP kinase was also detected in the region where *Mkp3* and *scleraxis*-positive progenitor cells were detected (Fig. 4D). However, in order to visualise this staining, the contrast had to be increased significantly, indicating that the levels of dpERK along the anterior and posterior edges of the dorsal sclerotome are very low, which is entirely consistent with MKP3 phosphatase activity in these cells.

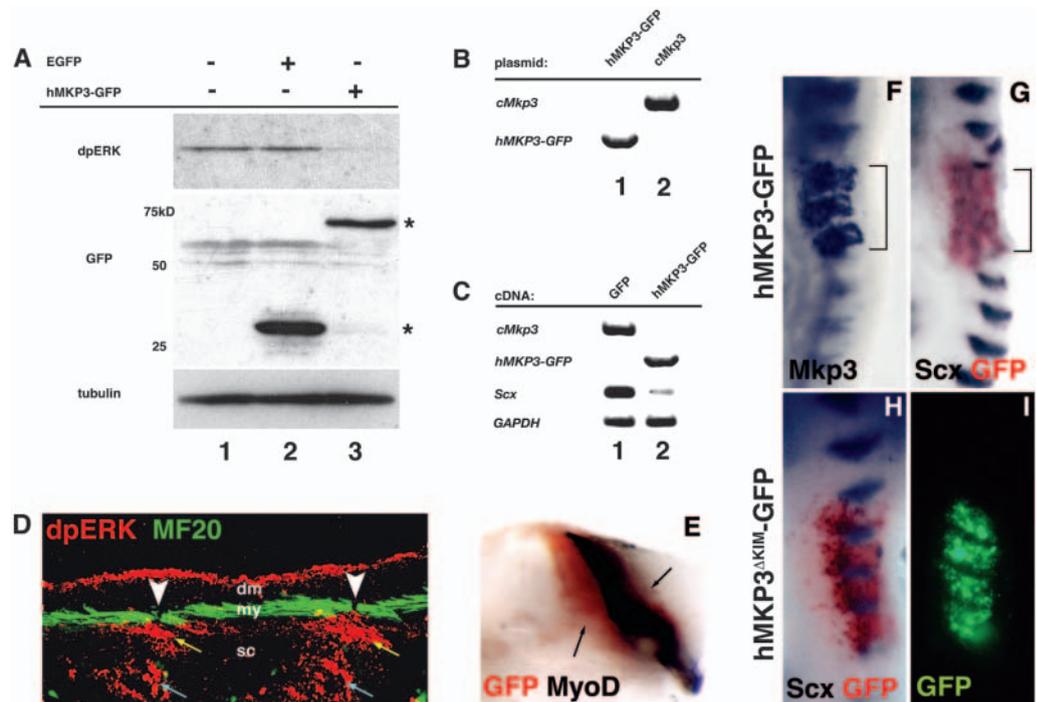## Ectopic MKP3 within somites results in loss of scleraxis positive progenitor cells

We next investigated how manipulating the levels of active ERK MAP kinase influenced somite patterning and in particular the specification of *scleraxis*-positive progenitor cells. Electroporation of the hMKP3-GFP fusion protein into somites of HH18 embryos resulted in high levels of *hMKP3-GFP* expression throughout the dermomyotome, myotome and dorsal

most part of the sclerotome, as visualised by detection of GFP and MyoD in sections (Fig. 4E). In situ hybridisation using the chick *Mkp3* probe, which crossreacted with human transcripts, also demonstrated high-level expression (Fig. 4F). In agreement with RT-PCR results, we found that expression of hMKP3-GFP led to a loss of *scleraxis* expression (Fig. 4G). The same result was obtained after expression of chick *Mkp3* from a different expression vector (data not shown). Expression of EGFP alone had no effect on *scleraxis* (Fig. 6F). To exclude the possibility that expression of the MKP3 phosphatase at high levels could affect non-specifically other phospho-proteins required for *scleraxis* expression we used a mutant of MKP3 that does not contain the conserved kinase-interaction motif 'KIM' (Nichols et al., 2000). This mutant protein has a normal basal activity in vitro but is unable to undergo catalytic activation in response to ERK2 or to inactivate ERK2 upon transfection into mammalian cells (Karlsson et al., 2004). Electroporation of the KIM mutant did not affect *scleraxis* expression in any of the embryos (Fig. 4H), even when expressed at high levels (Fig. 4I). These experiments suggest that active ERK MAP kinase, the levels of which are regulated by MKP3, is required for *scleraxis* expression in somitic progenitor cells.

Constitutive activation of ERK MAP kinase results in loss of *Mkp3* transcripts

Next, we wanted to investigate how high levels of dpERK would affect the expression of *Mkp3* and *scleraxis* (Figs 5, 6).

We have used a mutant form of MKK in which activating residues have been mutated to create a constitutively active kinase (MKK$^{E/E}$=caMEK1) (Cowley et al., 1994). Western blot analysis of somites or neural tube electroporated with a caMEK1 expression plasmid demonstrated the presence of very high levels of dpERK compared with control tissues (Fig. 5B). Ectopic *Mkp3* transcripts were detected in the developing neural tube as a result of raised levels of dpERK. In electroporated somites, however, caMEK1 expression resulted in the loss of *Mkp3* and *scleraxis* transcripts (Fig. 5A, Fig. 6D). This may indicate that a particular level of ERK signalling is required to drive transcription of these genes. Alternatively, because electroporation introduced the transgene into the dermomyotome and myotome as well as the dorsal sclerotome (Fig. 4E), it was conceivable that high dpERK activity in these compartments led to the loss of *Mkp3* by an indirect mechanism. To investigate this possibility, we used markers for these compartments and found that *Pax3* was unaffected, suggesting a normal dermomyotome (Fig. 5C). However, although loss of dpERK as a result of hMKP3-GFP electroporation had no apparent effect on the myotome, as shown by normal *MyoD* expression (Fig. 5D,E), raising the levels of active ERK MAP kinase by electroporation of caMEK1 caused a loss of *MyoD* transcripts (Fig. 5F). This was consistent with the idea that a MyoD-dependent signal could synergise with dpERK to regulate *Mkp3* and *scleraxis*. Indeed, we found that *Fgf4* expression, which is regulated by MyoD

Fig. 4. MKP3 regulates its own expression by regulating ERK MAP kinase. (A) Western blot of protein extracted from untreated somites (lane 1), somites electroporated with EGFP vector (lane 2) or electroporated with hMKP3-GFP vector (lane 3); 15 μg was loaded in each lane. Asterisks on the right identify the EGFP protein (lane 2) and the hMKP3-GFP fusion protein (lane 3). α-tubulin served as a loading control. (B) PCR performed on plasmid DNA with specific primers. Human MKP3-GFP plasmid was detected with hMKP3-GFP primers but not with cMkp3 primers (lane 1). Chick Mkp3 plasmid was detected with cMkp3 primers but not with hMKP3-GFP primers (lane 2). (C) RT-PCR on cDNA obtained from somites expressing EGFP vector (lane 1) or hMKP3-GFP fusion protein (lane 2). (B,C) Templates used indicated at the top, primers used indicated on the left. (D) Immunohistochemistry on a frontal section using MF20 antibody detecting myosin heavy chain (green) and dpERK anti-body detecting active phosphorylated ERK MAP kinase (red). White arrowheads indicate rostrocaudal boundaries between somites. Dorsal root ganglia indicated by a blue arrow; dorsal sclerotome region indicated by a yellow arrow. (E) Section of somites electroporated with a GFP vector (in red) and hybridised with a probe detecting MyoD (dark blue). Arrows indicate extent of tissue electroporated, including dermomyotome, myotome and dorsal sclerotome. (F-I) Manipulating dpERK levels in somites results in loss of *scleraxis* transcripts, the following vectors were electroporated: (F,G) hMKP3-GFP, (H,I) hMKP3$^{\Delta KIM}$-GFP. Single and double in situ hybridisation of electroporated embryos with the probes indicated on each panel. (F) *Mkp3*, bracket indicates detection of high levels of human transcripts, which crossreact; (G) *scleraxis* and hMKP3-GFP detected using a GFP probe (*n*=19/22); (H) *scleraxis* and hMKP3$^{\Delta KIM}$-GFP detected using a GFP probe (*n*=8/8); (I) GFP fluorescence.

(Iwahori et al., 2004), was affected (Fig. 5H). However, loss of MyoD was also observed after implanting a bead soaked in FGF4 or FGF8 (Fig. 5G, data not shown). In this situation, ectopic *Mkp3* and *scleraxis* transcripts were induced (Fig. 3A,B,E). This finding therefore suggests that the loss of *MyoD* does not correlate with the loss of *Mkp3* and *scleraxis*.

Mis-regulation of dpERK levels results in loss of *scleraxis* expression and affects rib formation

To investigate the effects of aberrant FGF/ERK MAP kinase signalling on somite differentiation and to examine the long-term consequences for *scleraxis*-positive progenitor cells, we used RCAS mediated mis-expression of sFREK:Fc, which would antagonise FGF signalling in many somites due to widespread infection (Fig. 6I). Alcian Blue staining revealed the loss of multiple rib skeletal elements on the infected side; however, at fairly low frequency possibly owing to limited diffusion of sFREK:Fc (Fig. 6H). Next, we wanted to affect dpERK levels more directly using MKP3-GFP and caMEK1 viral misexpression. Sections showed that RCAS infection was restricted to cells in the dermomyotome and myotome (Fig. 6J) and thus, mesenchymal cells in the sclerotome were not

targeted efficiently. Because hMKP3-GFP and caMEK1 act in a cell-autonomous fashion this was not a feasible approach. Instead, we used electroporation of hMKP3-GFP and caMEK1 expression plasmids (Fig. 4E) and even though effects were restricted to electroporated somites (typically two to three thoracic somites), we saw a dramatic phenotype. As shown before, decreasing dpERK levels by MKP3 resulted in the loss of *scleraxis* expression (Fig. 4C,G; Fig. 6A). At 10 days of development, distal ribs had failed to form from targeted somites in 60% of the embryos. We electroporated somites that gave rise to the first or the seventh rib (Fig. 6B,C). Increasing dpERK levels by caMEK1 also resulted in the loss of *scleraxis* expression and affected distal rib formation (60%; Fig. 6D,E). Electroporation of GFP alone did not disturb *scleraxis* expression or rib formation in any of the embryos analyzed
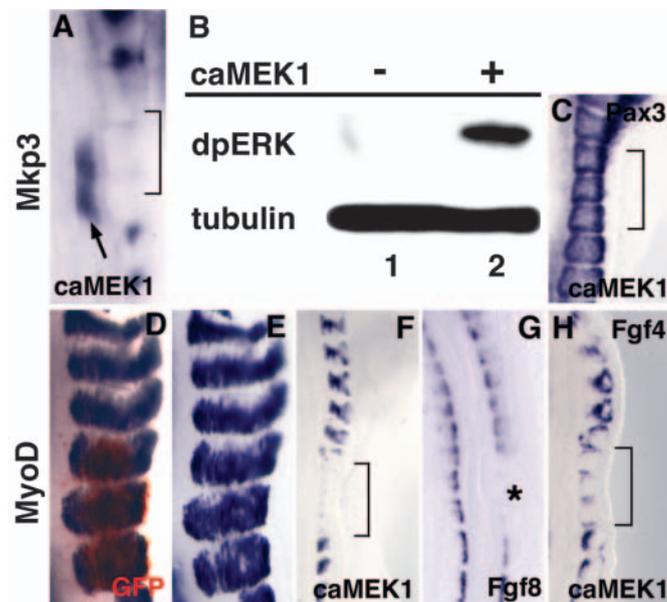

Fig. 5. High levels of dpERK activity in somites results in loss of *MyoD* and *Mkp3*. (A) In situ hybridisation for *Mkp3* after electroporation of a plasmid encoding caMEK1, a constitutively active form of MKK1; arrow indicates ectopic *Mkp3* transcripts in the neural tube, bracket indicates the loss of *Mkp3* transcripts in targeted somites (*n*=30/35). (B) Western blot detecting dpERK in somites electroporated with caMEK1 plasmid (+) compared with control somites (–); 7.5 μg of protein was loaded in each lane, compared with twice that amount in Fig. 3D and Fig. 4A. (D-G) In situ hybridisation for *MyoD*. (D) hMKP3-GFP electroporation has no effect on *MyoD* expression (*n*=16/16). INT/BCIP was used to detect GFP probe (red), it was washed out using methanol to visualise *MyoD* (E). (F) caMEK1 electroporation caused complete loss of *MyoD* transcripts (blue, indicated by bracket; *n*=10/15) but *Pax3* (C) was not affected (*n*=16/16). (G) FGF8 beads (asterisk) resulted in loss of *MyoD* in adjacent somites (*n*=7/11). (H) caMEK1 electroporation caused a significant loss of *Fgf4* transcripts (blue, indicated by bracket; *n*=13/18).
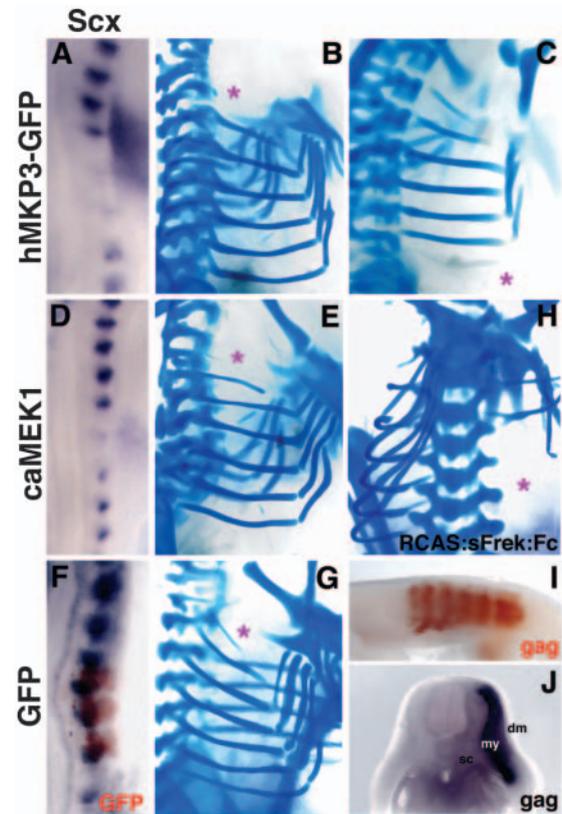
Fig. 6. Manipulating dpERK levels leads to loss of *scleraxis* expression and rib defects. (A,D,F) Whole-mount in situ hybridisation of (A,D) *scleraxis* (dark blue) and (F) *scleraxis* with GFP (red). (A) hMKP3-GFP electroporation and (D) caMEK1 electroporation resulted in loss of *scleraxis* transcripts (*n*=19/22 and *n*=10/14). (F) GFP electroporation had no effect (*n*=16/16). (B,C,E,G) Alcian Blue staining of cartilage. Loss of dpERK resulted in loss of the distal part of rib one (B, *n*=8/12) or rib seven (C, *n*=9/16), depending on the somites targeted. (E) High levels of dpERK caused loss of the distal part of rib one (*n*=9/15). (G) GFP alone had no effect on rib development (*n*=12/12). (H) Infection of thoracic somites with RCAS-sFREK:Fc, at day 10 of development, multiple ribs failed to form (*n*=2/16). (I) In situ hybridisation detecting RCAS gag transcripts 48 hours after infection (red). (J) Transverse section through RCAS infected somite demonstrates presence of transcripts predominantly in the dorsal somite. Asterisks indicate missing ribs (B,C,E,H) compared with rib present in control (G). dm, dermomyotome; my, myotome; sc, sclerotome.

(Fig. 6F,G), indicating that this phenotype is specifically due to perturbation of dpERK levels.

Discussion

Here, we describe the expression and regulation of the ERK MAP kinase specific phosphatase, MKP3. In addition, we investigate its function in somite patterning and differentiation. Our results suggest that regulation of ERK MAP kinase signal strength by MKP3 establishes a crucial level of FGF signalling important for appropriate expression of the effector gene *scleraxis*. Scleraxis has previously been implicated in the specification of axial tendon progenitors (Brent et al., 2003), and we present evidence that it may also be required for the differentiation of distal ribs.

Transcriptional regulation of *scleraxis* depends on negative feedback loops that control the level of dpERK

This study uncovered a function of the dual specificity ERK MAP kinase phosphatase, MKP3, for the specification of mesenchymal progenitors in the somite sclerotome. We showed that *Mkp3* was expressed in a twin-striped pattern, which closely matched the emergence of *scleraxis* transcripts along the anteroposterior somite edges (Fig. 1). This pattern suggested a link between the modulation of FGF signalling by MKP3 and *scleraxis* expression. We demonstrated that somitic expression of *Mkp3* in the dorsal sclerotome was itself dependent on active ERK MAP kinase. This implied that FGF signalling in dorsal sclerotome cells is modulated by a negative feedback loop, which involves MKP3 and ERK MAP kinase. Indeed, we found that the levels of *Mkp3* transcripts detected in response to FGF beads can cycle between extensive overexpression after a short exposure to complete loss of endogenous *Mkp3* message after 24 hours (Fig. 3A-C; data not shown). We showed by western blot analysis that this dynamic response correlated with an increase in active dpERK protein after 1 hour and the loss of dpERK after 24 hours (Fig. 3D). This suggests that high levels of MKP3 protein resulted in depletion of dpERK from somites, which then lead to a loss of further endogenous *Mkp3* transcription. This was confirmed by RT-PCR analysis (Fig. 4C). In mouse embryos, implanting an FGF4 bead into the primitive streak had similar effects after 24 hours because of expansive *Spry2* expression (Davidson et al., 2000) and it is likely that in chick somites sprouty and other negative regulators impact upon this feedback loop. Interestingly, the expression of *Mkp3* immediately around the bead was not affected by the feedback mechanism (Fig. 3C), as an ERK MAP kinase independent pathway, i.e. PI3-kinase (Fig. 2E) could also regulate *Mkp3* expression in response to FGF beads (Kawakami et al., 2003; Echevarria et al., 2005).

MKP3 is a cell-autonomous modifier of FGF signalling and this strongly suggested that FGFs signal to the dorsal sclerotome to control *scleraxis* expression. We also show that dpERK is localised in the region where *scleraxis* positive cells are found (Fig. 4D). It is possible that other signalling pathways cooperate with ERK MAP kinase and converge to control the spatiotemporal expression of *Mkp3* in developing somites (Moreno and Kintner, 2004; Rintelen et al., 2003; Tsang et al., 2004). For example, our results using caMEK1, which led to a loss of MyoD, would be consistent with the idea

that a MyoD-dependent factor contributes to the expression of *Mkp3* and *scleraxis* (Fig. 5F). However, MyoD was also lost after application of an FGF bead (Fig. 5G), which induced ectopic expression of *Mkp3* and *scleraxis*, and this argues against a MyoD-dependent mechanism. Furthermore, *scleraxis* is expressed in MyoD- and Myf5-null mice (Tajbakhsh et al., 1996; Brent et al., 2005). In mouse, FGF4 is important for *scleraxis* expression (Brent et al., 2005). We show that *Fgf4* expression is lost after caMEK1 treatment (Fig. 5H); this could provide a simple explanation for the loss of *scleraxis* under these conditions. However, *scleraxis* expression depended on ERK activity (Fig. 2L, Fig. 4C,G, Fig. 6A), which was directly stimulated in somites after caMEK1 electroporation (Fig. 4E). Therefore, loss of *MyoD* and *Fgf4* could not explain the loss of *scleraxis* transcription.

We have focused here on MKP3, which is one of many negative regulators of the MAP kinase transduction pathway. Other members of this group include Sef, Spred and Sprouty. Expression of Sef and Sprouty is induced by activation of the MAP kinase cascade itself, and as MKP3 regulates MAP kinase activity directly it could be pivotal in controlling these antagonists, which act at different levels in the pathway (Ozaki et al., 2001; Furthauer et al., 2002; Tsang et al., 2002; Yusoff et al., 2002; Kovalenko et al., 2003). This suggests that MKP3 acts at a crucial level in the FGF signal transduction cascade regulating all downstream events that depend on ERK MAP kinase, including activation of transcription factors and phosphorylation of cytoplasmic targets. Furthermore, other signalling cascades, including the retinoic acid and Wnt/β-catenin pathways, are able to regulate the expression of *Mkp3* in other tissues (Moreno and Kintner, 2004; Tsang et al., 2004). This provides a possible role for other pathways, yet to be described in somites, to limit *Mkp3* expression to the dorsal sclerotome and would explain how FGF responsive genes can be restricted.

In this study, overexpression experiments in chick embryos demonstrated the close interdependence of dpERK and MKP3, which established a tightly controlled level of active ERK MAP kinase in cells exposed to FGFs. There seem to be discrepancies between the FGF bead experiments and caMEK1 electroporation. *Mkp*3 was expressed when high levels of dpERK were present in response to a bead (Fig. 3A). Equally, caMEK1 induced an increase of dpERK but led to a loss of *Mkp3* transcription (Fig. 5A). The most likely explanation for these apparently conflicting results is our finding that the bead-mediated upregulation of *Mkp3* can go through ERK MAP kinase and PI3-kinase (Fig. 2D,E). By contrast, expression of *scleraxis* is probably dependent on dpERK only, and we and others have found that *scleraxis* is upregulated in response to an FGF bead after 5 hours (Fig. 3E) (Brent and Tabin, 2004). Electroporation of hMKP3-GFP led to loss of dpERK and concomitant loss of *scleraxis* (Fig. 4A,C,G). We propose that *scleraxis* can only be induced at a certain level of dpERK, set by the MKP3-ERK feedback loop. This is consistent with the delayed induction of *scleraxis* by FGF beads relative to *Mkp3* (Fig. 3E), which correlates with a specific level of dpERK (Fig. 3D) and with the observed loss of *scleraxis* when dpERK levels are either too high (Fig. 6D) or too low (Fig. 4C,G; Fig. 6A). In *Drosophila*, the *puckered* gene, a member of the same family as *Mkp3*, functions in a negative feedback loop to modulate JNK MAP kinase activity. In both *puckered* overexpression and

loss-of-function experiments, a similar defect in dorsal closure resulted, reminiscent of our data (Martin-Blanco et al., 1998). In addition, negative-feedback regulation has been proposed to confer multistability on ERK MAP kinase activity (Markevich et al., 2004) and the response of *scleraxis* to an intermediate level of dpERK would be in agreement with this model. Our finding that MKP3 is capable of inhibiting all downstream effectors involved in *scleraxis* induction, presumably by depleting active ERK MAP kinase, suggests that within the somite, the MKP3-dpERK negative feedback loop is crucial for establishing specific signal strength.

The function of MKP3 and scleraxis in distal rib specification

This work demonstrated a functional importance of MKP3 for the correct expression of *scleraxis*. This in turn is pivotal for the specification of cells in the dorsal sclerotome. *Scleraxis* marks both tendon and rib progenitors in the sclerotome of thoracic somites. Based on our data, we speculate that scleraxis functions in the specification of distal rib chondrocytes at an early stage for the following reasons. First, scleraxis has been shown to increase aggrecan expression and stimulate chondrogenesis in cell culture (Liu et al., 1997). Second, *scleraxis* is transiently co-expressed with *sox9*, a chondrogenic marker in rib primordia, in mouse at 12.5 dpc (Asou et al., 2002; Brent et al., 2005). However, after 13.5 dpc expression diverges, which we interpret as scleraxis acting at an early stage of rib specification. Similarly, in chick, *scleraxis* is no longer expressed in condensing ribs and the expression pattern is consistent with an early requirement for *scleraxis* in rib development (Brent et al., 2003). Third, when we altered the signal strength of ERK MAP kinase, distal ribs did not form (Fig. 6). Of the somitic markers analyzed, only *scleraxis* expression was consistently lost under these conditions. Fourth, in electroporated embryos, one rib was typically affected, consistent with the loss of *scleraxis* expression from the anterior border of one somite and the posterior border of the next (Fig. 6D). Thus, we speculate that one domain of *scleraxis* formed by two successive somites, gives rise to one rib structure. This is in agreement with experiments demonstrating that the distal rib arises through a process involving resegmentation (Aoyama and Asamoto, 2000).

The mechanism leading to rib loss remains to be investigated and could involve a failure of progenitor cells to become specified. For example, *scleraxis* may act together with BMP signalling and forkhead transcription factors in cell specification (Buchberger et al., 1998; Kramer et al., 2000; Sudo et al., 2001). Alternatively, progenitor cells may undergo apoptosis or they might fail to migrate. In this context, it is interesting to note that the migration of cells from the lateral somite into the somatopleure is dependent on the regulation of paxillin by ERK activity (Ishibe et al., 2004).

Interestingly, in mouse, the expression of *Fgf8*, *scleraxis* and *Mkp3* is different suggesting a species-specific change in the function of MKP3. In chick, *Fgf8* transcripts are found in the central myotome but in mice they colocalise with *scleraxis* at the rostral and caudal somite edges, indicating that FGF8 signals in an autocrine fashion (Crossley and Martin, 1995). In mouse, *Mkp3* is not expressed in the dorsal sclerotome but in the dermomyotome/myotome (Dickinson et al., 2002; Klock and Herrmann, 2002). Thus, it would be interesting to

investigate whether *Mkp3* knockout mice have normal ribs and tendons.

References

Aoyama, H. and Asamoto, K. (2000). The developmental fate of the rostral/caudal half of a somite for vertebra and rib formation: experimental confirmation of the resegmentation theory using chick-quail chimeras. *Mech. Dev.* **99**, 71-82.

Asou, Y., Nifuji, A., Tsuji, K., Shinomiya, K., Olson, E. N., Koopman, P. and Noda, M. (2002). Coordinated expression of scleraxis and Sox9 genes during embryonic development of tendons and cartilage. *J. Orthop. Res.* **20**, 827-833.

Brent, A. E. and Tabin, C. J. (2004). FGF acts directly on the somitic tendon progenitors through the Ets transcription factors Pea3 and Erm to regulate scleraxis expression. *Development* **131**, 3885-3896.

Brent, A. E., Schweitzer, R. and Tabin, C. J. (2003). A somitic compartment of tendon progenitors. *Cell* **113**, 235-248.

Brent, A. E., Braun, T. and Tabin, C. J. (2005). Genetic analysis of interactions between the somitic muscle, cartilage and tendon cell lineages during mouse development. *Development* **132**, 515-528.

Buchberger, A., Schwarzer, M., Brand, T., Pabst, O., Seidl, K. and Arnold, H. H. (1998). Chicken winged-helix transcription factor cFKH-1 prefigures axial and appendicular skeletal structures during chicken embryogenesis. *Dev. Dyn.* **212**, 94-101.

Buckingham, M. (2001). Skeletal muscle formation in vertebrates. *Curr. Opin. Genet. Dev.* **11**, 440-448.

Camps, M., Nichols, A., Gillieron, C., Antonsson, B., Muda, M., Chabert, C., Boschert, U. and Arkinstall, S. (1998). Catalytic activation of the phosphatase MKP-3 by ERK2 mitogen-activated protein kinase. *Science* **280**, 1262-1265.

Corson, L. B., Yamanaka, Y., Lai, K. M. and Rossant, J. (2003). Spatial and temporal patterns of ERK signaling during mouse embryogenesis. *Development* **130**, 4527-4537.

Cowley, S., Paterson, H., Kemp, P. and Marshall, C. J. (1994). Activation of MAP kinase kinase is necessary and sufficient for PC12 differentiation and for transformation of NIH 3T3 cells. *Cell* **77**, 841-852.

Crossley, P. H. and Martin, G. R. (1995). The mouse Fgf8 gene encodes a family of polypeptides and is expressed in regions that direct outgrowth and patterning in the developing embryo. *Development* **121**, 439-451.

Cserjesi, P., Brown, D., Ligon, K. L., Lyons, G. E., Copeland, N. G., Gilbert, D. J., Jenkins, N. A. and Olson, E. N. (1995). Scleraxis: a basic helix-loop-helix protein that prefigures skeletal formation during mouse embryogenesis. *Development* **121**, 1099-1110.

Davidson, B. P., Cheng, L., Kinder, S. J. and Tam, P. P. (2000). Exogenous FGF-4 can suppress anterior development in the mouse embryo during neurulation and early organogenesis. *Dev. Biol.* **221**, 41-52.

Davies, S. P., Reddy, H., Caivano, M. and Cohen, P. (2000). Specificity and mechanism of action of some commonly used protein kinase inhibitors. *Biochem. J.* **351**, 95-105.

Dickinson, R. J., Eblaghie, M. C., Keyse, S. M. and Morriss-Kay, G. M. (2002). Expression of the ERK-specific MAP kinase phosphatase PYST1/MKP3 in mouse embryos during morphogenesis and early organogenesis. *Mech. Dev.* **113**, 193-196.

Eblaghie, M. C., Lunn, J. S., Dickinson, R. J., Munsterberg, A. E., Sanz-Ezquerro, J. J., Farrell, E. R., Mathers, J., Keyse, S. M., Storey, K. and Tickle, C. (2003). Negative feedback regulation of FGF signaling levels by Pyst1/MKP3 in chick embryos. *Curr. Biol.* **13**, 1009-1018.

Echevarria, D., Martinez, S., Marques, S., Lucas-Teixeira, V. and Belo, J. A. (2005). Mkp3 is a negative feedback modulator of Fgf8 signaling in the mammalian isthmic organizer. *Dev. Biol.* **277**, 114-128.

Edom-Vovard, F., Bonnin, M. A. and Duprez, D. (2001). Misexpression of Fgf-4 in the chick limb inhibits myogenesis by down-regulating Frek expression. *Dev. Biol.* **233**, 56-71.

Development

Evans, D. J. (2003). Contribution of somitic cells to the avian ribs. *Dev. Biol.* **256**, 114-126.

Furthauer, M., Lin, W., Ang, S. L., Thisse, B. and Thisse, C. (2002). Sef is a feedback-induced antagonist of Ras/MAPK-mediated FGF signalling. *Nat. Cell Biol.* **4**, 170-174.

Groom, L. A., Sneddon, A. A., Alessi, D. R., Dowd, S. and Keyse, S. M. (1996). Differential regulation of the MAP, SAP and RK/p38 kinases by Pyst1, a novel cytosolic dual-specificity phosphatase. *EMBO J.* **15**, 3621-3632.

Hajihosseini, M. K., Lalioti, M. D., Arthaud, S., Burgar, H. R., Brown, J. M., Twigg, S. R., Wilkie, A. O. and Heath, J. K. (2004). Skeletal development is regulated by fibroblast growth factor receptor 1 signalling dynamics. *Development* **131**, 325-335.

Hamburger, V. and Hamilton, H. L. (1951). A series of normal stages in the development of the chick embryo. *J. Morphol.* **88**, 49-92.

Hanafusa, H., Torii, S., Yasunaga, T. and Nishida, E. (2002). Sprouty1 and Sprouty2 provide a control mechanism for the Ras/MAPK signaling pathway. *Nat. Cell Biol.* **4**, 850-858.

Hirao, A. and Aoyama, H. (2004). Somite development without influence of the surface ectoderm in the chick embryo: the compartments of a somite responsible for distal rib development. *Dev. Growth Differ.* **46**, 351-362.

Huang, R., Stolte, D., Kurz, H., Ehehalt, F., Cann, G. M., Stockdale, F. E., Patel, K. and Christ, B. (2003). Ventral axial organs regulate expression of myotomal Fgf-8 that influences rib development. *Dev. Biol.* **255**, 30-47.

Ishibe, S., Joly, D., Liu, Z. X. and Cantley, L. G. (2004). Paxillin serves as an ERK-regulated scaffold for coordinating FAK and Rac activation in epithelial morphogenesis. *Mol. Cell* **16**, 257-267.

Iwahori, A., Fraidenraich, D. and Basilico, C. (2004). A conserved enhancer element that drives FGF4 gene expression in the embryonic myotomes is synergistically activated by GATA and bHLH proteins. *Dev. Biol.* **270**, 525-537.

Karlsson, M., Mathers, J., Dickinson, R. J., Mandl, M. and Keyse, S. M. (2004). Both nuclear-cytoplasmic shuttling of the dual specificity phosphatase MKP-3 and its ability to anchor MAP kinase in the cytoplasm are mediated by a conserved nuclear export signal. *J. Biol. Chem.* **279**, 41882-41891.

Kawakami, Y., Rodriguez-Leon, J., Koth, C. M., Buscher, D., Itoh, T., Raya, A., Ng, J. K., Esteban, C. R., Takahashi, S., Henrique, D. et al. (2003). MKP3 mediates the cellular response to FGF8 signalling in the vertebrate limb. *Nat. Cell Biol.* **5**, 513-519.

Klock, A. and Herrmann, B. G. (2002). Cloning and expression of the mouse dual-specificity mitogen-activated protein (MAP) kinase phosphatase Mkp3 during mouse embryogenesis. *Mech. Dev.* **116**, 243-247.

Kouhara, H., Hadari, Y. R., Spivak-Kroizman, T., Schilling, J., Bar-Sagi, D., Lax, I. and Schlessinger, J. (1997). A lipid-anchored Grb2-binding protein that links FGF-receptor activation to the Ras/MAPK signaling pathway. *Cell* **89**, 693-702.

Kovalenko, D., Yang, X., Nadeau, R. J., Harkins, L. K. and Friesel, R. (2003). Sef inhibits fibroblast growth factor signaling by inhibiting FGFR1 tyrosine phosphorylation and subsequent ERK activation. *J. Biol. Chem.* **278**, 14087-14091.

Kramer, J., Hegert, C., Guan, K., Wobus, A. M., Muller, P. K. and Rohwedel, J. (2000). Embryonic stem cell-derived chondrogenic differentiation in vitro: activation by BMP-2 and BMP-4. *Mech. Dev.* **92**, 193-205.

Liu, Y., Watanabe, H., Nifuji, A., Yamada, Y., Olson, E. N. and Noda, M. (1997). Overexpression of a single helix-loop-helix-type transcription factor, scleraxis, enhances aggrecan gene expression in osteoblastic osteosarcoma ROS17/2.8 cells. *J. Biol. Chem.* **272**, 29880-29885.

Marics, I., Padilla, F., Guillemot, J. F., Scaal, M. and Marcelle, C. (2002). FGFR4 signaling is a necessary step in limb muscle differentiation. *Development* **129**, 4559-4569.

Markevich, N. I., Hoek, J. B. and Kholodenko, B. N. (2004). Signaling switches and bistability arising from multisite phosphorylation in protein kinase cascades. *J. Cell Biol.* **164**, 353-359.

Martin-Blanco, E., Gampel, A., Ring, J., Virdee, K., Kirov, N., Tolkovsky, A. M. and Martinez-Arias, A. (1998). puckered encodes a phosphatase that mediates a feedback loop regulating JNK activity during dorsal closure in Drosophila. *Genes Dev.* **12**, 557-570.

Minowada, G., Jarvis, L. A., Chi, C. L., Neubuser, A., Sun, X., Hacohen, N., Krasnow, M. A. and Martin, G. R. (1999). Vertebrate Sprouty genes are induced by FGF signaling and can cause chondrodysplasia when overexpressed. *Development* **126**, 4465-4475.

Moreno, T. A. and Kintner, C. (2004). Regulation of segmental patterning by retinoic acid signaling during Xenopus somitogenesis. *Dev. Cell* **6**, 205-218.

Muda, M., Theodosiou, A., Rodrigues, N., Boschert, U., Camps, M., Gillieron, C., Davies, K., Ashworth, A. and Arkinstall, S. (1996). The dual specificity phosphatases M3/6 and MKP-3 are highly selective for inactivation of distinct mitogen-activated protein kinases. *J. Biol. Chem.* **271**, 27205-27208.

Muda, M., Theodosiou, A., Gillieron, C., Smith, A., Chabert, C., Camps, M., Boschert, U., Rodrigues, N., Davies, K., Ashworth, A. et al. (1998). The mitogen-activated protein kinase phosphatase-3 N-terminal noncatalytic region is responsible for tight substrate binding and enzymatic specificity. *J. Biol. Chem.* **273**, 9323-9329.

Münsterberg, A. E., Kitajewski, J., Bumcrot, D. A., McMahon, A. P. and Lassar, A. B. (1995). Combinatorial signaling by Sonic hedgehog and Wnt family members induces myogenic bHLH gene expression in the somite. *Genes Dev.* **9**, 2911-2922.

Nichols, A., Camps, M., Gillieron, C., Chabert, C., Brunet, A., Wilsbacher, J., Cobb, M., Pouyssegur, J., Shaw, J. P. and Arkinstall, S. (2000). Substrate recognition domains within extracellular signal-regulated kinase mediate binding and catalytic activation of mitogen-activated protein kinase phosphatase-3. *J. Biol. Chem.* **275**, 24613-24621.

Niswander, L., Jeffrey, S., Martin, G. R. and Tickle, C. (1994). A positive feedback loop coordinates growth and patterning in the vertebrate limb. *Nature* **371**, 609-612.

Ozaki, K., Kadomoto, R., Asato, K., Tanimura, S., Itoh, N. and Kohno, M. (2001). ERK pathway positively regulates the expression of Sprouty genes. *Biochem. Biophys. Res. Commun.* **285**, 1084-1088.

Partanen, J., Schwartz, L. and Rossant, J. (1998). Opposite phenotypes of hypomorphic and Y766 phosphorylation site mutations reveal a function for Fgfr1 in anteroposterior patterning of mouse embryos. *Genes Dev.* **12**, 2332-2344.

Rintelen, F., Hafen, E. and Nairz, K. (2003). The Drosophila dual-specificity ERK phosphatase DMKP3 cooperates with the ERK tyrosine phosphatase PTP-ER. *Development* **130**, 3479-3490.

Sasaki, A., Taketomi, T., Kato, R., Saeki, K., Nonami, A., Sasaki, M., Kuriyama, M., Saito, N., Shibuya, M. and Yoshimura, A. (2003). Mammalian Sprouty4 suppresses Ras-independent ERK activation by binding to Raf1. *Nat. Cell Biol.* **5**, 427-432.

Sato, T. and Nakamura, H. (2004). The Fgf8 signal causes cerebellar differentiation by activating the Ras-ERK signaling pathway. *Development* **131**, 4275-4285.

Schmidt, M., Tanaka, M. and Münsterberg, A. E. (2000). Expression of b-catenin in the developing chick myotome is regulated by myogenic signals. *Development* **127**, 4105-4113.

Schweitzer, R., Chyung, J. H., Murtaugh, L. C., Brent, A. E., Rosen, V., Olson, E. N., Lassar, A. and Tabin, C. J. (2001). Analysis of the tendon cell fate using Scleraxis, a specific marker for tendons and ligaments. *Development* **128**, 3855-3866.

Storm, E. E., Rubenstein, J. L. and Martin, G. R. (2003). Dosage of Fgf8 determines whether cell survival is positively or negatively regulated in the developing forebrain. *Proc. Natl. Acad. Sci. USA* **100**, 1757-1762.

Sudo, H., Takahashi, Y., Tonegawa, A., Arase, Y., Aoyama, H., Mizutani-Koseki, Y., Moriya, H., Wilting, J., Christ, B. and Koseki, H. (2001). Inductive signals from the somatopleure mediated by bone morphogenetic proteins are essential for the formation of the sternal component of avian ribs. *Dev. Biol.* **232**, 284-300.

Tajbakhsh, S., Rocancourt, D. and Buckingham, M. (1996). Muscle progenitor cells failing to respond to positional cues adopt non-myogenic fates in myf-5 null mice. *Nature* **384**, 266-270.

Tallquist, M. D., Weismann, K. E., Hellstrom, M. and Soriano, P. (2000). Early myotome specification regulates PDGFA expression and axial skeleton development. *Development* **127**, 5059-5070.

Tsang, M., Friesel, R., Kudoh, T. and Dawid, I. B. (2002). Identification of Sef, a novel modulator of FGF signalling. *Nat. Cell Biol.* **4**, 165-169.

Tsang, M., Maegawa, S., Kiang, A., Habas, R., Weinberg, E. and Dawid, I. B. (2004). A role for MKP3 in axial patterning of the zebrafish embryo. *Development* **131**, 2769-2779.

Yang, X., Dormann, D., Münsterberg, A. E. and Weijer, C. J. (2002). Cell movement patterns during gastrulation in the chick are controlled by positive and negative chemotaxis mediated by FGF4 and FGF8. *Dev. Cell* **3**, 425-437.

Yusoff, P., Lao, D. H., Ong, S. H., Wong, E. S., Lim, J., Lo, T. L., Leong, H. F., Fong, C. W. and Guy, G. R. (2002). Sprouty2 inhibits the Ras/MAP kinase pathway by inhibiting the activation of Raf. *J. Biol. Chem.* **277**, 3195-3201.